Nuclear Engineering and Design 426 (2024) 113361



Contents lists available at ScienceDirect

Nuclear Engineering and Design

journal homepage: www.elsevier.com/locate/nucengdes





Scaling approach and forced-circulation flow patterns in the liquid metal-cooled reactor-pool experiment E-SCAPE

Katrien Van Tichelen [a,c,*], Fabio Mirelli [a], Matteo Greco [a], Yann Bartosiewicz [b], William D'haeseleer [c]

[a] SCK CEN, Institute for Advanced Nuclear Systems, Boeretang 200, 2400 Mol, Belgium
[b] UCLouvain, Institute of Mechanics, Materials, and Civil Engineering (iMMC), Thermodynamics and Fluid Mechanics Division, Place du Levant 2, 1348 Louvain-la-Neuve, Belgium
[c] KU Leuven, Applied Mechanics and Energy Conversion, Celestijnenlaan 300, 3001 Leuven, Belgium

ARTICLE INFO

Keywords:
Liquid metal-cooled reactor
Integral test facility
Thermal hydraulic scale model
Lead bismuth eutectic
Flow pattern

ABSTRACT

The validation of decay heat removal systems and the characterization of thermal hydraulic phenomena in the plena of the liquid metal-cooled, pool-type research reactor MYRRHA, under design at SCK CEN, the Belgian Nuclear Research Centre, is accomplished by experiments and numerical investigations. For this purpose, the E-SCAPE facility at SCK CEN is a thermal hydraulic 1/6-scale 3-D model of the primary system of MYRRHA, with an electrical core simulator, and cooled with Lead Bismuth Eutectic (LBE). Its scaling is based on the preservation of the overall system behavior and the reproduction of the major thermal hydraulic phenomena under decay heat removal conditions. Specific attention in the scaling approach is given to stratification phenomena in the upper plenum and the mixing effect associated with jets entering the plena. From steady-state isothermal operation in forced circulation, experimental information is obtained on the pressure losses in the system. The relation between the pressure loss in the core and above core structure, and the level difference between the lower and upper plenum is confirmed. From hot plug experiments, using temperature as a flow tracer, a large amount of information on the flow patterns in forced circulation mode is generated. For instance, a clear difference can be observed in the behavior of pump jets entering the lower plenum between the high and low flow rate cases. One can also see that the LBE that exits the core, is going upwards through the above core structure before distributing radially in the uppermost fluid layers. From these layers, the fluid goes downward in the upper plenum towards the inlet windows of the heat exchangers.

1. Introduction

This paper is part of a series that deals with thermal hydraulic experiments performed in the E-SCAPE (European Scaled Pool Experiment) facility at SCK CEN, the Belgian Nuclear Research Centre (Van Tichelen et al., 2015). They support the development of Heavy Liquid Metal nuclear technology in general and in particular that of the MYRRHA Accelerator Driven System (Aït Abderrahim et al., 2021). MYRRHA includes a flexible fast-neutron spectrum, pool-type research reactor cooled by Lead Bismuth Eutectic (LBE).

The MYRRHA design version 1.2 (Aït Abderrahim, 2011) is at the basis of this paper and is presented in Fig. 1 and Table 1. The reactor has all its primary components submerged in the liquid metal inside the reactor vessel ①. The diaphragm ② separating the upper and lower plena, is hanging from the main flange of the reactor vessel. It consists of a vertical cylindrical shell that is closed at its lower end by two horizontal circular plates. The upper plenum (UP) consists of the space inside the cylindrical shell above the top horizontal plate. The annular space between the cylindrical shell and the vessel connects to the large volume under the bottom horizontal plate; together they are the so-called the 'lower plenum' (LP). The space between the two horizontal circular plates is the intermediate plenum. The core ③ is inserted in the core barrel ④, a perforated tube that allows the hot LBE coolant leaving the core to reach the upper plenum and establish the first free surface. The Above Core Structure (ACS) ⑤ allows handling the control and safety rods, accommodates instrumentation and forces the fluid to go out through the lateral openings in the core barrel. The hot LBE from the upper plenum enters in four primary heat exchangers (PHXs) ⑥. The PHXs interface with the secondary cooling system, consisting of four

* Corresponding author at: SCK CEN, Institute for Advanced Nuclear Systems, Boeretang 200, 2400 Mol, Belgium.
E-mail address: katrien.van.tichelen@sckcen.be (K. Van Tichelen).

https://doi.org/10.1016/j.nucengdes.2024.113361
Received 3 May 2024; Received in revised form 30 May 2024; Accepted 30 May 2024
Available online 7 June 2024
0029-5493/© 2024 Elsevier B.V. All rights are reserved, including those for text and data mining, AI training, and similar technologies.

Nomenclature

Abbreviations

ACS	Above Core Structure
BP	Bypass
CFD	Computational Fluid Dynamics
DHR	Decay Heat Removal
FC	Forced Circulation
HP	Hot Plug
LBE	Lead Bismuth Eutectic
LFR	Lead-cooled Fast Reactor
LP	Lower Plenum
NC	Natural Circulation
PHX	Primary Heat Exchanger
P&ID	Piping and Instrumentation Diagram
SFR	Sodium-cooled Fast Reactor
TC	Thermocouple
UP	Upper Plenum

Roman letters

a	area [m^2]
A	area scale
Bi	Biot number
c_p	specific heat at constant pressure of the fluid [J/(kg.K)]
d	hydraulic diameter of the fluid channel [m]
Eu	Euler number
f	Darcy friction coefficient
F	Friction number
Fo	Fourier number
Fr	Froude number
g	magnitude of the gravitational acceleration [m/s^2]
h	heat transfer coefficient [$W/(m^2.K)$]
H	height of the stratified fluid [m]
HS	Heat Source number
k	thermal conductivity [W/(m.K)]
K	minor loss coefficient
l	length of the fluid channel [m]
L	length ratio (axial scale) level difference of core and PHX thermal centers [m]
$\dot{m}$	mass flow rate [kg/s]
Nu	Nusselt number
p	pressure [Pa or mbar]
Pe	Péclet number
Pr	Prandtl number
$\dot{q}$	volumetric heat generation in the fluid [W/m^3]
$\dot{q}_s$	volumetric heat generation in the solid [W/m^3]
Q	heating rate [W]
Re	Reynolds number
Ri	Richardson number
St	Modified Stanton number
t	time [s]
T	temperature [K or °C]
T^*	Time Ratio number
u	fluid velocity [m/s]
x, y, z	coordinate system

Subscripts

0	reference section
eq	equivalent
i	i^{th} section of the flow loop
in	at core inlet
h	hot fluid section
L	facility including loops
m	experimental model
p	reactor prototype
R	ratio between model and prototype
s	solid
tot	total

Greek letters

α	thermal diffusivity of the fluid
β	thermal expansion coefficient of the fluid [1/K]
δ	conduction depth [m]
Δ	difference
ν	kinematic viscosity of the fluid [m^2/s]
ρ	mass density of the fluid [kg/m^3]
σ_{stat}	statistical deviation
σ_{inst}	accuracy of the instrumentation
σ_{ADC}	uncertainty due to analogue-to-digital conversion
σ_{tot}	total uncertainty
τ_{well}	time constant of a thermocouple in a thermowell [s]
Ψ	dimensionless group

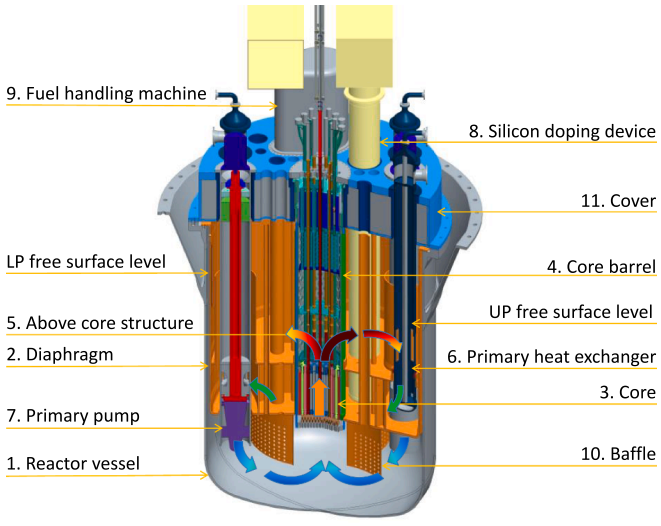

Fig. 1. Main components and coolant flow path in the MYRRHA reactor (design version 1.2).

independent water-steam circuits connecting to four aero-condensers. After leaving the PHXs, the cold LBE reaches two primary pumps ⑦ and is delivered to the lower plenum where it establishes the second free surface in the annular space between the diaphragm and the vessel. In the upper plenum the silicon doping devices ⑧ allow the nuclear transmutation doping and the in-vessel fuel handling machines ⑨ are responsible for the loading and unloading of the fuel assemblies in the core. The baffle ⑩, a metal plate with a butterfly shape that is attached to the diaphragm and punched with holes, limits the work area for recovery of lost fuel assemblies. All the penetrations are held in position and fixed by the cover ⑪.

Table 1 includes parameters for nominal operation and in decay heat removal mode, the latter both in forced circulation and in natural circulation. The design has been further optimized in the past years leading to design version 1.8 (De Bruyn, 2021). Despite modifications to individual components and their size, its overall configuration is unaltered, except for the silicon doping devices that have been removed from the system. The results and conclusions obtained remain very relevant for the latest design version.

Using passive systems to achieve safety functions is one of the guiding principles of the MYRRHA design. Natural circulation in the

Table 1
Parameters and scaling ratios for forced (FC) and natural (NC) circulation.

			MYRRHA v.1.2			E-SCAPE DESIGN		SCALING		
Parameter		Unit	Nominal operation	DHR & FC	DHR & NC	DHR & FC	DHR & NC	$\Psi_{R,ideal}$	$\Psi_{R,DHR\&FC}$	$\Psi_{R,DHR\&NC}$
GEOMETRY										
d_{core}	$\sqrt{\frac{4a_0}{\pi}}$	m	1.45	1.45	1.45	0.25	0.25	0.172	**0.172**	**0.172**
d_{vessel}		m	7.98	7.98	7.98	1.38	1.38	0.172	**0.173**	**0.173**
a_{core}	a_0	m^2	1.65	1.65	1.65	0.05	0.05	0.030	**0.030**	**0.030**
l_{core}	l_0	m	2.03	2.03	2.03	0.37	0.37	0.172	**0.182**	**0.182**
l_{UP}	l_{UP}	m	2.39	2.39	2.39	0.41	0.41	0.172	**0.172**	**0.172**
l_h	l_h	m	1.00	1.00	1.00	0.17	0.17	0.172	**0.172**	**0.172**
L	L	m	1.00	1.00	1.00	3.50	3.50	0.172	*3.500*	*3.500*
PROCESS DATA										
Q	$\dot{q}a_0l_0$	W	1.10×10^8	7.80×10^6	7.80×10^6	1.02×10^5	1.02×10^5	0.012	**0.013**	**0.013**
$\dot{\mathbf{q}}$		W/m^3	3.28×10^7	2.33×10^6	2.33×10^6	5.61×10^6	5.61×10^6	2.408	**2.408**	**2.408**
$\dot{\mathbf{m}}_{\mathbf{tot}}$	$\rho u_0 a_0$	kg/s	9374.90	9374.90	493.15	116.58	6.16	0.012	**0.012**	**0.012**
T_{in}		°C	270	270	270	180	180	–	–	–
ΔT_{core}	ΔT_0	°C	80.44	5.70	108.40	5.89	111.47	1.000	**1.032**	**1.028**
u_{core}	u_0	m/s	0.55	0.55	0.03	0.23	0.01	0.415	**0.414**	**0.415**
$\Delta p_{vessel\text{-}HX}$		Pa	2.50×10^5	2.50×10^5	1.26×10^3	4.32×10^4	2.20×10^2	0.172	**0.173**	**0.174**
$\Delta p_{pump\ and\ HX\ loops+HX}$		Pa	5.00×10^4	5.00×10^4	1.38×10^2	4.57×10^5	4.85×10^3	0.172	*9.135*	*35.140*
INTEGRAL SYSTEM										
HS	$\frac{\dot{q}l_0}{\rho c_p u_0 \Delta T_0}$	–	1.00	1.00	1.00	1.00	1.00	1.000	**1.000**	**1.000**
Eu	$\frac{\Delta p_{vessel-HX}}{\rho u_0^2}$	–	80.55	80.55	146.94	80.50	146.89	1.000	**0.999**	**1.000**
Ri	$\frac{g\beta\Delta T_0 l_h}{u_0^2}$	–	0.34	0.02	164.00	0.02	166.73	1.000	**1.029**	**1.017**
Ri_L	$\frac{g\beta\Delta T_0 L}{u_0^2}$	–	0.34	0.02	164.00	0.50	3384.62	1.000	20.88	*20.638*
Eu_L	$\frac{\Delta p}{\rho u_0^2}$	–	96.66	96.66	163.01	931.09	3384.62	1.000	*9.633*	*20.764*
Ri_L/Eu_L		–	0.003	0.0002	1.01	0.0005	1.00	1	2.168	**0.994**
T*	$\frac{L}{u_0}$	s	1.83	1.83	34.77	15.48	293.10	0.415	*8.462*	*8.429*
UPPER PLENUM										
Ri_{UP}	$\frac{g\beta\Delta T_0 l_{UP}}{u_0^2}$	–	0.80	0.06	391.87	0.06	397.45	1.000	**1.026**	**1.014**
Re_{UP}	$\frac{u_0 d_{core}}{\nu}$	–	4.16×10^6	4.16×10^6	2.19×10^5	2.28×10^5	1.20×10^4	1.000	0.055	0.055
Pe_{UP}	$\frac{u_0 d_{core}}{\alpha}$	–	1.05×10^5	1.05×10^5	5.54×10^3	8.67×10^3	4.58×10^2	1.000	0.082	0.083
Fr_{UP}	$u_0/\sqrt{gl_{UP}}$	–	0.11	0.11	0.01	0.11	0.01	1.000	**0.997**	**1.001**
T^*_{UP}	$\frac{l_{UP}}{u_0}$	s	4.37	4.37	83.09	1.82	34.42	0.415	**0.416**	**0.414**

primary system is the chosen option in terms of decay heat removal (DHR), keeping temperatures in the core within the safety limits and maintaining structural integrity of the coolant boundaries. The MYRRHA PHXs and secondary cooling system serve as prime DHR system in case of accidental events. The second decay heat removal function is performed by a reactor vessel auxiliary cooling system, based on water cooling of the reactor vessel external wall. Both systems rely on natural circulation in the reactor pool and their operational feasibility needs to be confirmed.

Thermal hydraulic phenomena occurring in the upper and lower plena of the reactor pool must be properly understood for structural integrity assessment and design optimization. This requires a good knowledge of convection patterns (e.g. flow distribution, free surface velocities), flow mixing (resulting e.g. in thermal striping[1]) and thermal stratification in operational and accidental conditions. Under forced circulation conditions, velocity and temperature depend mostly on the coolant flow rate. In natural circulation, flow rate and velocities depend on the temperature distribution and vice versa. Both flow regimes must be characterized in detail to support design and safety analysis.

The validation of DHR systems and the characterization of thermal hydraulic phenomena can be accomplished by experiments and numerical investigations. This requires the development of test facilities, that simulate the expected pool-type environment as closely as possible, as well as the creation of an experimental database to be used for the validation of the computational models used in design and safety analysis.

For pool-type Sodium-cooled Fast Reactors (SFRs), a natural circulation test using the Phenix reactor and the shutdown heat removal tests performed at the Experimental Breeder Reactor EBR-II are the topic of international benchmarks in IAEA coordinated research projects to validate state-of-the-art computational models (IAEA, 2013; 2017). The number of measurement data for code validation obtained from these reactor experiments is however limited as reactor instrumentation is installed for operational monitoring.

Because of their advantages in terms of cost, ease of operation and measurement, water scale models have been and are being used to study the thermal hydraulic behavior of new designs of liquid metal reactors.

[1] Thermal striping is characterized by oscillatory mixing of non-isothermal coolant streams and is a potential cause of thermal fatigue damage in structural materials.

The basis of water-sodium thermal hydraulic similarity was set by Grewal et al (Grewal and Gluekler, 1982). Water models have been used to study natural circulation, to assess the performance of DHR systems and to investigate phenomena occurring in the upper and lower plena of SFRs in Germany (Weinberg et al., 1996), France (Tenchine, 2010), India (Mente et al., 2014) and Japan (Takeda et al., 1993; Murakami et al., 2015; Ono, et al., 2017). Recently, the French Alternative Energies and Atomic Energy Commission (CEA) in France performed gas entrainment experiments in the 1/6-scale mockup MICAS of the upper plenum of the ASTRID SFR connected to the PLATEAU water facility (Guenadou et al., 2021). Temperature and flow patterns are measured in detail to generate experimental databases for the validation of multi-dimensional models including Computational Fluid Dynamics (CFD).

Although scaling laws make using water very relevant, the low Prandtl number of water compared to liquid metals might lead to differences for specific phenomena such as thermal stratification (Grewal and Gluekler, 1982). To verify the conclusions based on water experiments for SFRs, a limited number of separate-effect experiments with liquid metal have been performed (Lorenz and Howard, 1977; Vidil et al., 1988; Ieda et al., 1990; Tanaka et al., 1990). Tanaka compared nondimensional temperature gradients at the stratification interface in water and sodium tests and concluded that small-scale sodium experiments underestimate the temperature gradient, whereas the nondimensional temperature gradient in water tests is slightly higher than the one measured in real SFRs: a result of the influence of the Péclet number.

To support the development of the MYRRHA LBE-cooled reactor, SCK CEN relies mainly on three test facilities for the investigation of natural and forced circulation and of phenomena occurring in the plena.

The von Karman Institute for Fluid Dynamics in a collaboration with SCK CEN, is operating a 1/5-scale water model of the MYRRHA reactor, called **MYRRHABELLE** (Planquart and Van Tichelen, 2019). It is a full Plexiglas model of the primary system and combines the upper and lower plenum separated by a diaphragm, an electrical core simulator and scale models of heat exchangers and pumps. The transparent coolant and structural material allow optical access for instrumentation (e.g. for particle image velocimetry). The complete model enables the investigation of the transient behavior of the complete primary system and at the same time the detailed analysis of the flow field in specific regions in the reactor pool.

In the development of Lead fast reactor (LFR)-type systems, the **CIRCE** facility at ENEA, Italy, is intensively used for the analysis of natural circulation cooling modes and the transition from forced to natural circulation (Lorusso et al., 2021). For this purpose, CIRCE employs a scaling that preserves the height differences between the thermal center of heat source and heat sink as in the reactor (i.e. the driving force in natural circulation) and only scales the transversal dimensions. The representation of the flow topology on the other hand is limited as the facility only contains one core channel, heat exchanger and pump.

The **E-SCAPE** facility at SCK CEN is a thermal hydraulic 1/6-scale model of the primary system of the MYRRHA reactor, with an electrical core simulator, cooled with LBE. With its dense network of instrumentation, E-SCAPE provides detailed experimental feedback to the designers on the natural and forced circulation flow patterns. The E-SCAPE and MYRRHABELLE facilities are complementary: they represent the same reactor design at similar scales but use different fluids. This makes them well suited to investigate the Péclet number effect as explained later.

The present work reports results from thermal hydraulic experiments performed in the E-SCAPE facility in the frame of the Horizon 2020 framework program MYRTE of the European Commission (European Commission, 2015). This paper explains the rationale for the scaling approach used to design the facility in more detail compared to (Van Tichelen et al., 2015) in §2. The facility and its instrumentation are described in §3. The test matrix is presented in §4. Experimental results from isothermal and hot-plug operation are discussed in §5.

2. Scaling approach

A scaled test facility should be designed in such a way as to preserve the overall system behavior and reproduce major thermal hydraulic phenomena under relevant conditions. In principle, to obtain total 'dynamic and energetic similarity', it is required that each dimensionless number describing a major phenomenon (resulting from a Buckingham-Π analysis) for the scaled-down model equals that of the prototype. Regrettably, however, reality does not allow to obtain full similarity. The objective of a 'judicious' scaling analysis as discussed below, is to approximate full similarity as close as reasonably possible. This entails to understand the shortcomings and to account for the caveats before transposing the experimental results obtained with the scaled-down model for 'predicting' real physical behavior in the full-scale reactor.

2.1. Natural circulation

2.1.1. Integral system behavior

In the context of liquid–metal fast reactors, Ishii and Kataoka (Ishii and Kataoka, 1984) developed similarity criteria for single-phase natural circulation. These are derived from the integral 1-D conservation equations along the entire flow path in the reactor (see Supplemental file: Section 1). Six dimensionless numbers are obtained from non-dimensionalizing equations for mass, momentum and energy conservation in the fluid and solids:

$$\Psi_1 = Ri \equiv \frac{g\beta\Delta T_0 l_0}{u_0^2} = \frac{\text{buoyancy}}{\text{inertia force}} \quad \text{Richardson number} \tag{1}$$

$$\Psi_2 = HS_i \equiv \left(\frac{\dot{q}_s l_0}{\rho c_{ps} u_0 \Delta T_0}\right)_i = \frac{\text{heat source}}{\text{axial energy change}} \quad \text{Heat Source number} \tag{2}$$

$$\Psi_3 = F_i \equiv \left(\frac{fl}{d} + K\right)_i = \frac{\text{friction}}{\text{inertia force}} \quad \text{Friction number} \tag{3}$$

$$\Psi_4 = St_i \equiv \left(\frac{4hl_0}{\rho c_p u_0 d}\right)_i = \frac{\text{wall convection}}{\text{axial convection}} \quad \text{Modified Stanton number} \tag{4}$$

$$\Psi_5 = Bi_i \equiv \left(\frac{h\delta}{k_s}\right)_i = \frac{\text{wall convection}}{\text{conduction}} \quad \text{Biot number} \tag{5}$$

$$\Psi_6 = T_i^* \equiv \left(\frac{l_0/u_0}{\delta^2/\alpha_s}\right)_i = \frac{\text{transport time}}{\text{conduction time}} \quad \text{Time Ratio number} \tag{6}$$

with $\alpha = k/\rho c_p$, the thermal diffusivity of the fluid. The subscript "0" refers to the chosen reference section (e.g. the heated section or reactor core) and the subscript "s" means solid. The index "i" indicates the ith section of the flow loop (e.g. reactor core, heat exchanger, piping system).

In addition to the dynamic similarity groups, two geometrical similarity groups are defined:

$$\Psi_7 = L_i = l_i/l_0 \quad \text{Axial scale} \tag{7}$$

$$\Psi_8 = A_i = a_i/a_0 \quad \text{Flow area scale} \tag{8}$$

Selecting the heated section in the model or the reactor core in the prototype as the reference section, Ishii and Kataoka furthermore obtain reference scales for u_0 and ΔT_0 from the steady-state solution of the

conservation equations:

$$\Delta T_0 = \frac{\dot{q}_{s0} l_0}{\rho c_p u_0} \left(\frac{a_{s0}}{a_0} \right) \tag{9}$$

$$u_0 = \left\{ \frac{\beta \left(\frac{\dot{q}_{s0} l_0}{\rho c_p} \right) l_h \left(\frac{a_{s0}}{a_0} \right)}{\frac{1}{2g} \sum_i \left(F_i / A_i^2 \right)} \right\}^{1/3} \tag{10}$$

As said above, for similarity between the prototype and the model, all dimensionless groups must meet the following requirement:

$$\Psi_R \equiv \frac{\Psi_m}{\Psi_p} = 1 \tag{11}$$

From the continuity equation and the momentum conservation equation, the following geometrical similarity criteria can be derived:

$$\mathrm{A}_{iR} \equiv \frac{(a_i/a_0)_m}{(a_i/a_0)_p} = 1 \tag{12}$$

$$\left(\sum_i L_i / A_i \right)_R = 1 \tag{13}$$

$$L_{hR} = 1 \tag{14}$$

From the dynamic similarity conditions, one obtains that:

$$\left(\sum_i F_i / A_i^2 \right)_R = 1 \tag{15}$$

For simplicity, Ishii and Kataoka assume length similarities and uniform scaling, which is somewhat stricter than eqs. (12), (13) and (14):

$$\mathrm{L}_{iR} \equiv \frac{(l_i/l_0)_m}{(l_i/l_0)_p} = 1 \tag{16}$$

$$a_{0R} = l_{0R}^2 \tag{17}$$

Moreover, they assume that the same material is used for structures in the model as in the prototype. With these conditions, the ratios of reference velocities and temperatures become:

$$u_{0R} = \frac{u_{0m}}{u_{0p}} = \left\{ \dot{q}_{0R} \left(\frac{\beta}{\rho c_p} \right)_R \left(\frac{\delta_{0R}}{d_{0R}} \right) l_{0R}^2 \right\}^{1/3} \tag{18}$$

$$\Delta T_{0R} = \frac{\Delta T_{0m}}{\Delta T_{0p}} = \dot{q}_{0R} \left(\frac{1}{\rho c_p} \right)_R \frac{l_{0R}}{u_{0R}} \frac{\delta_{0R}}{d_{0R}} \tag{19}$$

If one substitutes Eq. (19) in the definition of the Richardson number, one can see that $\mathrm{Ri}_R = 1$ is equivalent to Eq. (18). Therefore, the correct scaling of velocity satisfies the Richardson number requirement automatically.

The energy similarity conditions require that:

$$T^*_{iR} = l_R / \left(u_R \delta_{iR}^2 \right) = 1 \Leftrightarrow \delta_{iR} = \delta_R = \sqrt{u_R / l_R} \tag{20}$$

$$\mathrm{HS}_{iR} = \left(\rho c_p \right)_R d_{0R} / \delta_{0R} = 1 \Leftrightarrow d_{0R} = d_R = \frac{\delta_R}{\left(\rho c_p \right)_R} = \frac{1}{\left(\rho c_p \right)_R} \sqrt{l_R / u_R} \tag{21}$$

$$\mathrm{Bi}_{iR} = h_R \delta_{iR} = 1 \Leftrightarrow h_{iR} = h_R = \sqrt{u_R / l_R} \tag{22}$$

$\mathrm{St}_{iR} = 1$ is automatically satisfied if the above criteria can be achieved. The time ratio scales the speed of transport processes in fluid and solid. The Biot number is the ratio of thermal resistance for conduction in a solid to the resistance for convection at the surface of the solid. The heat source number is important for the temperature in the solid and the overall energy level of the system. The Biot and Stanton number are related to the boundary condition at the fluid–solid interface and contain a heat transfer coefficient. Whereas Eqs. (20) and (21) lead to additional geometrical constraints, Eq. (22) imposes a condition on the heat transfer coefficient h. The latter is however a result from the fluid properties and flow conditions, expressed in a correlation for the Nusselt number $Nu \equiv hd/k$, and cannot be set. Using appropriate expressions for Nu, one obtains constraints on operational and design parameters that are quite different from Eq. (22). Hence, similarity of Biot and Stanton is difficult to realize. As a result of their similarity distortion, the system adjusts to a different temperature drop in the thermal boundary layer, but the overall flow and energy distribution will not be strongly affected in slow transients typical of a natural circulation system. Therefore, Ishii and Kataoka conclude it is most important to prioritize the similarities of the Richardson, the Heat Source and the Euler numbers.

One can arrive to the same conclusions by ignoring solid structures and fluid–solid heat transfer from the start (Ieda et al., 1993; Eguchi et al., 1997) (see Supplemental file: Section 1). If heat fluxes on the surface of a structure, e.g. on the surface of fuel pins or heat exchangers tubes, can be exactly imposed in the model, similar to the prototype, the energy equations in the solid and the boundary conditions at the fluid–solid interface disappear from the analysis. As a result, the modified Stanton, Biot and Time Ratio numbers do not appear in the analysis. The Heat Source number can be redefined as:

$$\Psi_2 = HS_i \equiv \left(\frac{\dot{q} l_0}{\rho c_p u_0 \Delta T_0} \right)_i = \left(\frac{Q}{\rho c_p u_0 \Delta T_0 a_0} \right)_i \tag{23}$$

Selecting the ratio of the reference velocity and temperature ratios now as:

$$u_{0R} = \left(\frac{\beta}{\rho c_p l_0} \right)_R^{1/3} Q_R^{1/3} \tag{24}$$

$$\Delta T_{0R} = \left(\beta \rho^2 c_p^2 l_0^5 \right)_R^{-1/3} Q_R^{2/3} \tag{25}$$

and introducing these in Eqs. (1) and (23), one can derive that Richardson and Heat Source similarity are automatically respected. Recall that the subscript R refers to the ratio between the model and the prototype. Hence, Eqs. (24) and (25) can also be used to upscale results from the model to the prototype. One has to take into account that the time scale will be shifted by the factor $t_R = l_{0R}/u_{0R}$.

The friction number is related to the more commonly used Euler number (with Δp the pressure difference in the fluid):

$$\Psi_{3eq} = Eu_i \equiv \frac{\Delta p_i}{\rho u_i^2} = \frac{1}{2} \left(\frac{fl}{d} + K \right)_i = \frac{1}{2} F_i \quad \text{(Euler number)} \tag{26}$$

For the similarity of the Euler number, Eq. (26) tells that a possible loss of frictional pressure drop in a scaled down model can be compensated for by a minor loss coefficient, e.g. using an orifice. However, the Euler number has to be matched over the entire range of operation (e.g. from full flow to natural circulation conditions in a loss-of-flow experiment). As the friction factor f cannot be considered constant but becomes very dependent on the Reynolds number (see Eq. (27)) when the latter becomes very small (typically below 4000), the Euler number does not remain constant. Grewal and Glueker recognize that as a result, respecting Euler similarity cannot be accomplished exactly for very small Reynolds numbers (Grewal and Gluekler, 1982).

Similarity conditions regarding the Reynolds and the Péclet numbers,

$$\Psi_9 = Re_i \equiv \left(\frac{u_0 l_0}{\nu}\right)_i = \frac{\text{inertia force}}{\text{viscous force}} \quad \text{(Reynolds number)} \tag{27}$$

$$\Psi_{10} = Pe_i \equiv \left(\frac{u_0 l_0}{\alpha}\right)_i = \frac{\text{axial convection}}{\text{axial conduction}} \quad \text{(Peclet number)} \tag{28}$$

are often neglected in integral system analysis. Also Ishii and Kataoka do not explicitly include viscous dissipation in the momentum equation (leading to the Re −similarity condition) or thermal conduction (leading to the Pe −similarity condition) in the fluid energy equation. Several authors have investigated the effects of violating Reynolds and Péclet similarities. Takeda (1993), Eguchi et al. (1997) and Ieda et al. (1993) concluded that for integral system analysis, Reynolds and Péclet similarity can be neglected, as long as the flow remains turbulent. Note that the Péclet number can be considered as a Prandtl-weighted Reynolds number since $Pe \equiv Re \times Pr$ with $Pr \equiv \nu/\alpha$ a material characteristic of the fluid.

2.1.2. Mixing in large stratified volumes

Since relatively large coolant temperature differences can exist in the components of fast reactors, local buoyancy driven flows can occur in these components. These local thermal hydraulic phenomena can influence the integral system behavior. Of particular interest is the upper plenum where strong thermal stratification can occur. Local similarity parameters characteristic for thermal stratification, can be derived from 3-D conservation equations in the upper plenum: Ri_{UP}, Re_{UP} and Pe_{UP} numbers following a similar process as in §2.1.1 (Ieda et al., 1993) (see Supplemental file: Section 2). Their definitions are identical to Eqs. (1), (27) and (28), but now using the upper plenum height l_{UP} as reference length:

$$Ri_{UP} = \frac{g\beta\Delta T_0 l_{UP}}{u_0^2} \tag{29}$$

$$Re_{UP} = \frac{u_0 l_{UP}}{\nu} = \left(\frac{Q\beta l_{UP}^2}{\nu^3 \rho c_p}\right)^{1/3} \tag{30}$$

$$Pe_{UP} = \frac{u_0 l_{UP}}{\alpha} = \left(\frac{Q\beta l_{UP}^2}{\alpha^3 \rho c_p}\right)^{1/3} \tag{31}$$

In the reactor plena, shear losses can be assumed to be small which makes Re_{UP} similarity less important. Thermal diffusion, in the non-dimensionalized equations represented by Pe_{UP}, however, plays an important role in the energy equation for thermally stratified conditions. The influence of Pe_{UP} is also clear from experimental investigations (Tanaka et al., 1990).

Inside stable stratified volumes, jets become the primary source of mixing (Peterson, 1994). This is the case in the upper plenum where buoyant jets are entering upwards from the reactor core or through the holes in the ACS. Peterson derived scaling criteria for vertical buoyant jet mixing in stratified systems (Peterson et al., 1998). For forced or inertia-dominated jets, the jet height to diameter ratio H/d_{jet} determines the entrainment into the jet. Here H is the height of the stratified fluid and equals l_{UP} in the upper plenum. If this aspect ratio is preserved, as is the case in uniform scaling (see Eq. (17)), similar mixing can be expected with full scale and reduced scale jets. For buoyant jets, it is not only necessary to preserve the aspect ratio, but also the jet Richardson number:

$$Ri_{jet} = \frac{(\rho_{UP} - \rho_{jet}) g d_{jet}}{\rho_{UP} u_{jet}^2} \tag{32}$$

where ρ_{jet} the jet entry density and u_{jet} the jet entry velocity. Moreover, if both are preserved, also the transition from forced to buoyant jet behavior scales properly.

Following the multi-level scaling approach presented in (Ishii et al., 1998), the scaling in E-SCAPE is firstly carried out with the objective to preserve the integral system behavior, prioritizing Ri, HS_i and Eu_i defined in §2.1.1. Second, the local phenomena in the upper plenum are reproduced as closely as possible. From their definition, one can derive that the Richardson numbers in the upper plenum Ri_{UP} and for the jet Ri_{jet} are automatically preserved when the integral scaling criteria are fulfilled (Ishii et al., 1998). Consequently, only the similarity condition on the Péclet number in the upper plenum ($Pe_{UP,R} = 1$) represents an additional scaling requirement.

2.1.3. Limits on scaling similarity

Respecting Péclet and Richardson similarity simultaneously is very challenging and often practically impossible. Fig. 2 (top) shows the ratios $Pe_{UP,R}$ and $Re_{UP,R}$ for $Ri_{UP,R} = Ri_R = 1$ for both an LBE and water scale model as function of the scaling factor l_{0R}. In order to keep temperature differences in measurable ranges, $\Delta T_{0R} = 1$ is set as an additional requirement. The reference LBE temperature is set at 270 °C; the water temperature is 27 °C. These are typical operational temperatures in the E-SCAPE (LBE) and MYRRHABELLE (water) facilities and the MYRRHA reactor (LBE). The ratios for MYRRHABELLE (water) and E-SCAPE (LBE) test facilities are indicated as well. It has to be noted that for MYRRHABELLE, $\Delta T_{0R} = 0.2$. Higher values of the ratio are not possible due to the power limitations in MYRRHABELLE.

In a medium-scale water model with Richardson similarity (e.g. $\Delta l_{0R} \approx 0.2$), the distortion in $Re_{UP,R}$ is in the order of 5.10^{-2}, while the distortion in $Pe_{UP,R}$ is about 10. For a medium-scale LBE model (e.g. E-SCAPE), the distortion in $Re_{UP,R}$ and $Pe_{UP,R}$ is in the order of 10^{-1}. The selection of the appropriate model size and simulant fluid is a balance

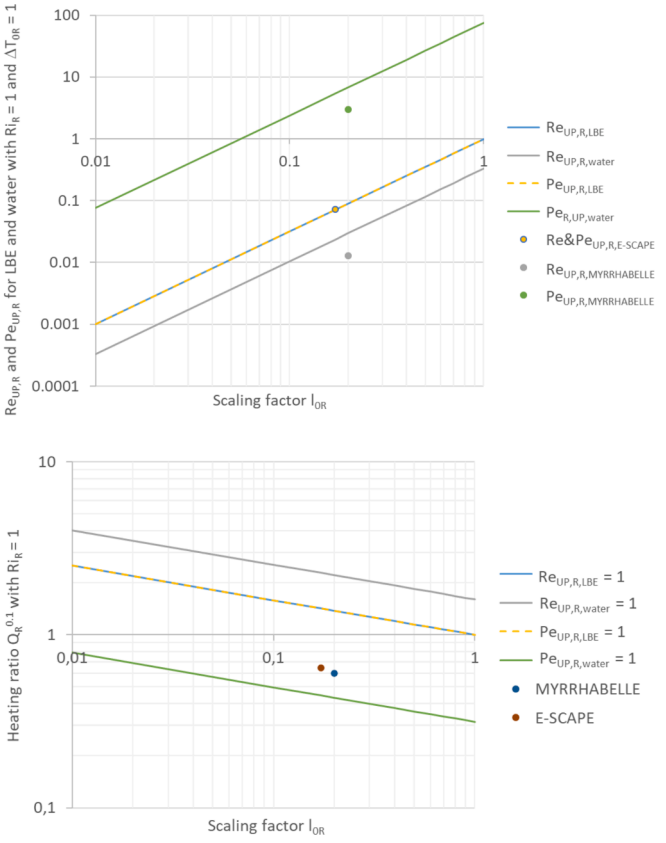

Fig. 2. $Re_{UP,R}$ and $Pe_{UP,R}$ for $Ri_R = 1$ and $\Delta T_{0R} = 1$ for an LBE and a water scale model (top) and heating ratio Q_R necessary to preserve upper plenum Reynolds and Péclet ratios for $Ri_R = 1$ (bottom).

between similarity requirements, practical limitations and project boundary conditions. In a medium-scale model $Re_{UP,R}$ is generally smaller than in the prototype but falls into the same (turbulent) regime in both model and prototype, while this is not necessarily the case in a small-scale experiment. Another advantage of a medium-scale model is that the geometrical similarity can better maintained than in a small-scale model. The Péclet number of medium-scale model experiments is larger than in reactor prototype conditions for water experiments and smaller for liquid–metal experiments. The Péclet number of water models can be reduced by reducing the heating ratio Q_R. This, however, at the same reduces ΔT_{0R} and $Re_{UP,R}$, as can be seen for MYRRHABELLE.

Again using Eqs. (30) and (31), Fig. 2 (bottom) gives the heating ratio Q_R that is necessary to preserve $Re_{UP,R}$ and $Pe_{UP,R}$ in the upper plenum for $Ri_R = 1$. Maximum power densities in the core are limited by practical considerations. This makes it impossible to reach the high heating ratios necessary to preserve *Re* and *Pe* in a medium-scale liquid–metal experiment. At the same time, heating rates should be high enough to lead to temperature differences that are measurable with acceptable accuracy. This complicates the preservation of $Pe_{UP,R}$ for medium-scale water experiments. Moreover, the low power ratios required for $Pe_{UP,R} = 1$ in water would lead to large distortion in $Re_{UP,R}$. Therefore, Ieda et al advises that investigations should be conducted comparing the results of medium-scale water and LBE experiments (Ieda et al., 1993). SCK CEN follows this advice with the MYRRHABELLE and E-SCAPE test facilities.

2.1.4. Scale model with the prototype fluid

If the model and the prototype have the same working fluid and the same temperature, Eqs. (24) and (25) reduce to:

$$u_{0R} = (Q_R/l_{0R})^{1/3} \tag{33}$$

$$\Delta T_{0R} = {l_{0R}}^{-5/3} Q_R^{2/3} \tag{34}$$

while preserving Reynolds and Péclet similarity requires (from Eqs. (30) and (31)):

$$Q_R = l_{0R}^{-2} \tag{35}$$

When introducing Eq. (35) in (33) and (34), one can see that similarity of all nondimensional numbers would not only lead to very high fluid velocities but would result in unacceptable values for ΔT_0. Relaxing the requirements on Reynolds and Péclet similarity, makes it possible to preserve ΔT_0, while keeping power density, velocity and time ratios t_R within acceptable boundaries:

$$\Delta T_{0R} = 1 \Longrightarrow Q_R = {l_{0R}}^{5/2} \Longrightarrow \dot{q}_R = l_{0R}^{-1/2} \Longrightarrow u_{0,R} = {l_{0R}}^{1/2} \Longrightarrow t_R = {l_{0R}}^{1/2} \tag{36}$$

2.2. Forced circulation

In single-phase forced circulation, when buoyancy forces become negligible, the momentum and energy equation are not coupled and similarity of the Richardson number is no longer mandatory. Euler and Heat Source number similarity remains important.

The flow in the plena is determined by the Froude, Reynolds and Péclet number (Guenadou et al., 2015). The Froude number:

$$Fr = u_0/\sqrt{g l_0} \tag{37}$$

relates the flow inertia to the gravitational pressure head as a result of the presence of a free surface of the fluid with a cover gas above.

2.2.1. Scale model with the prototype fluid

If the model and the prototype have the same working fluid and the same temperature, respecting Froude similarity results in the following relation:

$$u_{0R} = {l_{0R}}^{1/2} \tag{38}$$

It is impossible to fulfill Froude, Reynolds and Péclet similarity simultaneously. However, if Reynolds and Péclet numbers are large, their corresponding terms vanish from the conservation equations. Assuming $\Delta T_{0R} = 1$, heat source similarity again requires:

$$Q_R = {l_{0R}}^{5/2} \tag{39}$$

Eqs. (38) and (39) are identical to Eqs. (36).

2.3. E-SCAPE scaling

2.3.1. Choice of the model fluid

As advised in (Ieda et al., 1993), two test facilities have been developed that are geometrically similar to the MYRRHA reactor design, in order to investigate its integral system behavior and the phenomena occurring in the reactor plena. The MYRRHABELLE facility uses water as simulant fluid; in the E-SCAPE facility the prototype coolant LBE is used.

As the verification of DHR by natural circulation through the PHXs is one of the major objectives of the facilities, the scaling of both facilities is mostly based on the preservation of Richardson and Heat Source similarities in natural circulation as described in §2.1. From Fig. 2, one can observe the distortion in Reynolds and Péclet similarity in both facilities. The use of different fluids allows to investigate the effect of the Péclet similarity distortion as *Pe* for water experiments is higher and for LBE experiments is lower than in the reactor prototype.

The use of water has the advantage of posing far less practical challenges and enabling the use of established optical measurement techniques. The use of LBE, on the other hand, makes it possible to keep temperatures similar to the prototype ($\Delta T_{0R} \approx 1$) and allows to gain valuable operational experience with liquid–metal coolants.

2.3.2. Scaling factor

In addition to the similarity conditions, technological considerations such as core power density, total LBE inventory and standard pressure vessel dimensions have determined the geometrical scaling factor of E-SCAPE to be $l_{0R} = 1/5.8 = 0.172$. To the maximum possible extent the same geometrical scaling factor is used for all components, uniform in all directions. Pressure loss and heat exchange in the reactor vessel are mostly concentrated in the core region, in the PHXs and the pump regions. As it is practically impossible to correctly scale all dimensions of these complex components, only their inlet and outlet areas and lengths are scaled with l_{0R} while internally they are treated as 'black boxes'. The Euler number of the core region is respected by adding orifices at the model core inlet to match the loss of frictional pressure drop in the scale model. The core power determined by eq. (36) or (39) is provided by electrical heaters, distributed to match the power profile of the reactor as closely as possible.

For the PHX and pump regions, a particular approach is taken in E-SCAPE. The PHX inlet and pump outlet sections are scaled geometrically and their position in the vessel is preserved. Also the external dimensions of the PHX and pump channels from the cover, through the upper plenum and down to the lower plenum are respected, but space limitations force to position the actual pumps and heat exchangers (HXs) outside the vessel (see Fig. 3). They are placed in two external loops positioned above the main vessel and connecting to the PHX and pump channels. Despite the change in configuration, they still provide the correct boundary conditions to the main vessel in both steady-state forced and natural circulation conditions. The HXs remove the core power and provide the correct LBE inlet temperatures. In forced circulation, the pumps provide the scaled flow rates to the main vessel through the pump outlet sections following eq. (38). In natural circulation, the position of the HXs above the main vessel results in an increased level difference *L* between their thermal centers and that of the

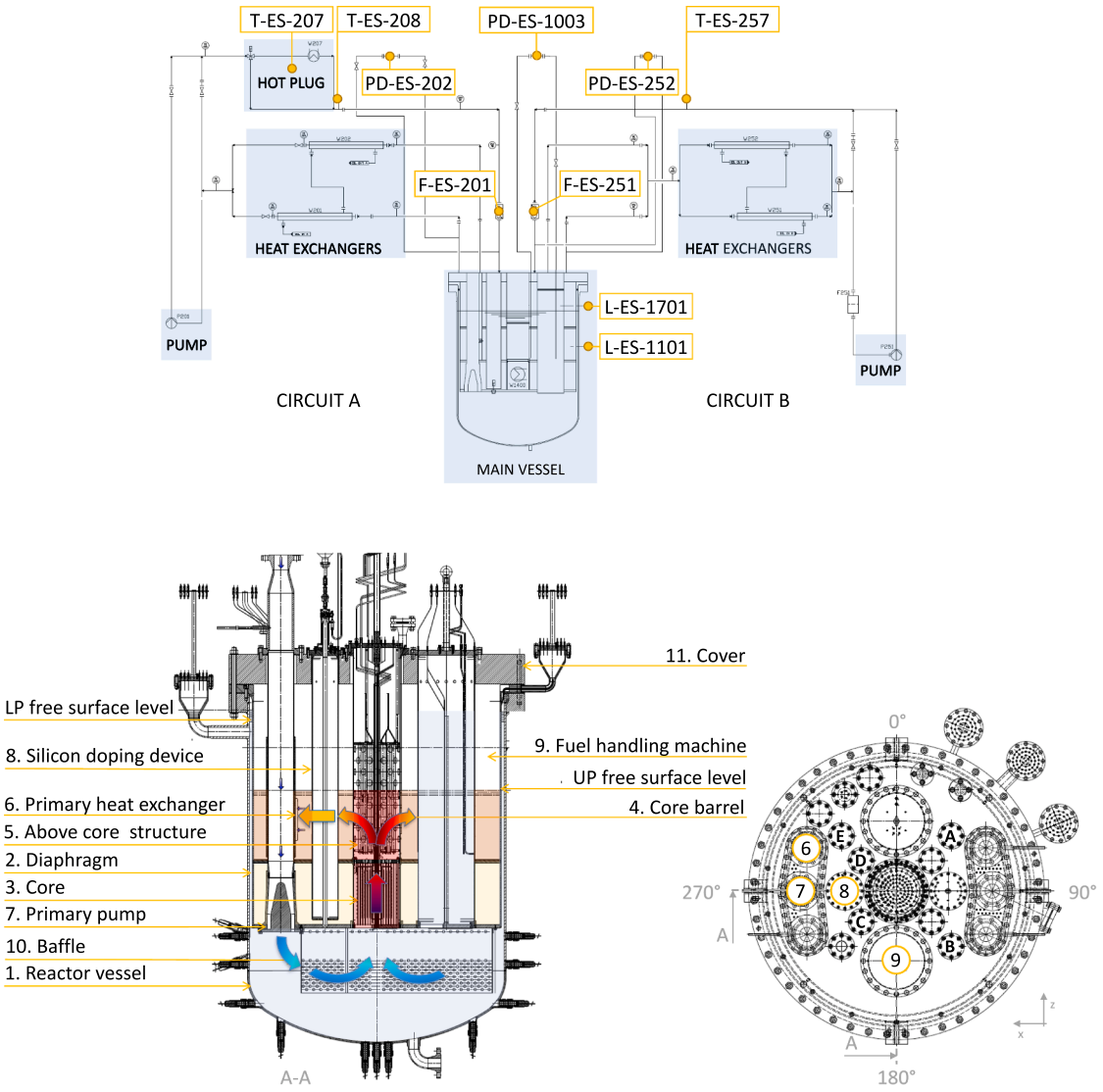

Fig. 3. E-SCAPE – Simplified primary system P&ID (top) and zoom on the main components and coolant flow path in the vessel (bottom).

core, increasing the buoyancy driving force (see Supplemental file: Section 3). To obtain the correctly scaled flow rates, the pressure losses in the external loops are increased as well to restore the balance. One can define a Richardson number and Euler number for the complete facility, including the external loops, as:

$$Ri_L \equiv \frac{g\beta\Delta T_0 L}{u_0^2} \tag{40}$$

$$Eu_L \equiv \frac{\Delta p}{\rho v_0^2} = \frac{1}{2}\left[\sum_{vessel}\left(\frac{fl}{D_H}+K\right)_i\left(\frac{a_0}{a_i}\right)^2 + \sum_{pumpand\ HXloops}\left(\frac{fl}{D_H}+K\right)_i\left(\frac{a_0}{a_i}\right)^2\right] \tag{41}$$

The balance between buoyancy head and pressure losses is guaranteed when:

$$\rho g\beta\Delta T_0 L = \frac{\rho v_0^2}{2}\left[\sum_{vessel}\left(\frac{fl}{D_H}+K\right)_i\left(\frac{a_0}{a_i}\right)^2 + \sum_{pumpand\ HXloops}\left(\frac{fl}{D_H}+K\right)_i\left(\frac{a_0}{a_i}\right)^2\right] \Leftrightarrow \frac{Ri_L}{Eu_L} = 1 \tag{42}$$

Naturally, by adding the loops, the LBE total inventory and hence the (thermal) inertia of the system and the turnover time of the flow increase. The LBE inventory of 1.9 m^3 in the vessel increases with 0.4 m^3 in the loops. This has an effect on the transient behavior of the system (slowing down thermal transients).

In steady state, the Richardson number defined for the main vessel based on l_0 using Eq. (1), remains respected. Respecting Richardson and Heat Source similarity with $\Delta T_{0R} = 1$ and $l_{0R} = 0.172$ results in the following scaling factors for core power and core power density:

$$Q_R = {l_{0R}}^{5/2} = 0.012 \Longrightarrow \dot{q}_R = l_{0R}^{-1/2} = 2.41 \tag{43}$$

The high power density ratio makes it impossible to scale MYRRHA's nominal operating power of 110 MW_{th}. As the focus of the investigations is on decay heat removal, a decay heat rate of 7 % of the nominal power is used as reference value (representative of the decay heat immediately after shutdown). This leads to a desired nominal operating power of 102 kW and a power density of 5610 kW/m^3 for E-SCAPE. With these values, ΔT_0 in steady-state natural circulation with decay heat power is the same in the model and in the prototype. In steady-state forced circulation, ΔT_0 in the model facility is much lower than in MYRRHA in nominal power conditions. However, as the flow is driven by the pumps, buoyancy is not important in nominal operation and respecting the Richardson number is not necessary. ΔT_0 measured in the experimental model has to be multiplied with $(7\%)^{-1} = 14.3$ with to obtain the expected values in MYRRHA in nominal power conditions.

The selected scaling factors for dimensions, temperature and power lead to distortion of the Péclet similarity in the upper plenum ($Pe_{UP,R} \approx 10^{-1}$) which can influence stratification in this component. From Tanaka (Tanaka et al., 1990) one can conclude that the nondimensional temperature gradient in the experiment is expected to be smaller than in the prototype as a result of an increased importance of conductive heat transport over convective transport.

For what concerns jets in the upper plenum and pump jets, the uniform geometrical scaling respects the jet height to diameter ratio. The jet Richardson number is preserved by the integral scaling approach.

Despite all efforts, not all experimental results can be transposed to reactor conditions as similarity of all dimensionless numbers is not achievable for all the physical phenomena, especially in transient conditions. In such cases, the results will be used to validate multidimensional computer models which are used in the reactor design.

3. E-SCAPE facility

3.1. Facility description

The E-SCAPE facility is a thermal hydraulic 1/6-scale 3-D model of the primary system of MYRRHA design version 1.2 cooled with LBE. Fig. 3 shows a simplified P&ID of the primary system of E-SCAPE with a zoom on the main vessel ①. Scaled replica of all main components are placed in the main vessel maintaining geometric similarity. The target design parameters of the E-SCAPE facility compared to the reference values of MYRRHA are reported in Table 1. Here, all pressure loss data are estimated values. The scaling ratio Ψ_R is included for both forced and natural circulation in DHR mode. The format indicates whether the E-SCAPE ratio approaches the ideal value from the theoretical scaling following §2 (**bold**), deviates within an acceptable range (normal) or deviates largely (*italic*). In forced circulation, buoyancy is not important and hence, the integral Richardson number is not relevant. The effect of the deviations of the Reynolds and Péclet numbers is already discussed in §2.1.1.

Electrical heaters simulate the nuclear core ③. The total power is given by 9 electrical heaters mounted spirally on 6 metal cylinders: the 5 internal cylinders represent the active core region; the 6th cylinder is in the core bypass (BP) region and has one heater able to supply 10 % of the total power. The BP power was set to correspond to the heating of the LBE due to Polonium activation and pump inefficiency. In the facility, the total core power is limited to 91.2 kW. The upper core grid at the outlet of the core represents the core support plate and provides the correct, scaled LBE velocities at the core outlet. The lower grid at the inlet of the core makes for the total pressure drop over the core to be representative of the scaled MYRRHA value. The ACS ⑤, an hexagonal array of rods, and core barrel ④ are similar to MYRRHA.

Contrary to MYRRHA, E-SCAPE is equipped with external primary cooling circuits, accommodating two pumps (5 bar – 20.4 m^3/h at 1057 rpm), two times two heat exchangers (4 x 30 kW) and six throttle valves, providing the correct boundary conditions to the main vessel in steady-state forced and natural circulation conditions. In natural circulation operation, the pumps in the two circuits can be isolated from the flow path with the LBE flowing through natural circulation bypasses, eliminating the pressure losses in the pump. In the main vessel, primary pumps ⑦ and PHXs ⑥ are simulated by dummy channels with openings scaled in size and position. The pump channels are thermally insulated from the upper plenum and the exit shapes are conform the MYRRHA version 1.2 design with a pump hub in the center.

The two external circuits are not identical. A three-way valve in primary circuit A allows the instantaneous introduction of a 20 l hot volume (hot plug – HP) of LBE in the main vessel for using temperature as a flow tracer. A Y-type filter in circuit B with a 50 μm wire mesh removes solid impurities from the LBE. The total length of the two circuits together is around 65 m. The nominal size of the piping is 3″. A cover gas pressure of 4.5 bar is maintained in the vessel through an Argon blanket, to prevent oxygen ingress and to guarantee the complete filling of the external circuits.

In MYRRHA, water at 16 bar is used as secondary coolant. The water is in saturation with a constant temperature of 201.4 °C. Because of ease of operation, thermal oil (Duratherm, 2023) is used as secondary coolant in the heat exchangers of E-SCAPE. Two secondary oil circuits with temperature between 125.0 °C and 200.0 °C remove the heat generated by the core in the primary system and evacuate it to the environment through two air coolers. Oil flow rates are high to minimize oil temperature increase. A control system opens the louvers and sets the fan speed of the air coolers to cool down the oil in the circuits and establish either a prescribed LBE inlet temperature (between 180.0 °C and 200.0 °C) into the main vessel or a fixed oil inlet temperature in the heat exchangers.

3.2. Instrumentation

E-SCAPE has a dense network of instrumentation to have a good characterization of the thermal hydraulic phenomena to support the validation of system analysis and CFD codes (see Fig. 3).

In each primary circuit, the LBE mass flow rate (F-ES-201/251) is measured using a Micro Motion ELITE Coriolis flow meter (accuracy ± 0.1 % of the read value). Pressure differences between the inlet and outlet of the main vessel, measured immediately above the vessel cover in the two circuits A and B (PD-ES-202/252) are recorded using two Rosemount 3051 differential pressure transmitter (accuracy ± 2.5 mbar). Oil volumetric flow rates are measured in both cooling loops using a Rosemount Vortex flow meter (accuracy ± 0.65 % of the read value).

In the main vessel, pressure sensing probes connecting to a Rosemount 3051 differential pressure transmitter (accuracy ± 0.21 mbar) provide the pressure difference between a point in the lower plenum and a point in the upper plenum at the same height (PD-ES-1003). In isothermal conditions, this pressure difference between plena equals the hydraulic pressure loss of the LBE between the inlet of the core and the outlet of the core barrel. Because of the particular design of MYRRHA and hence E-SCAPE, it also equals the level difference between the plena multiplied with the LBE density and the gravitational constant:

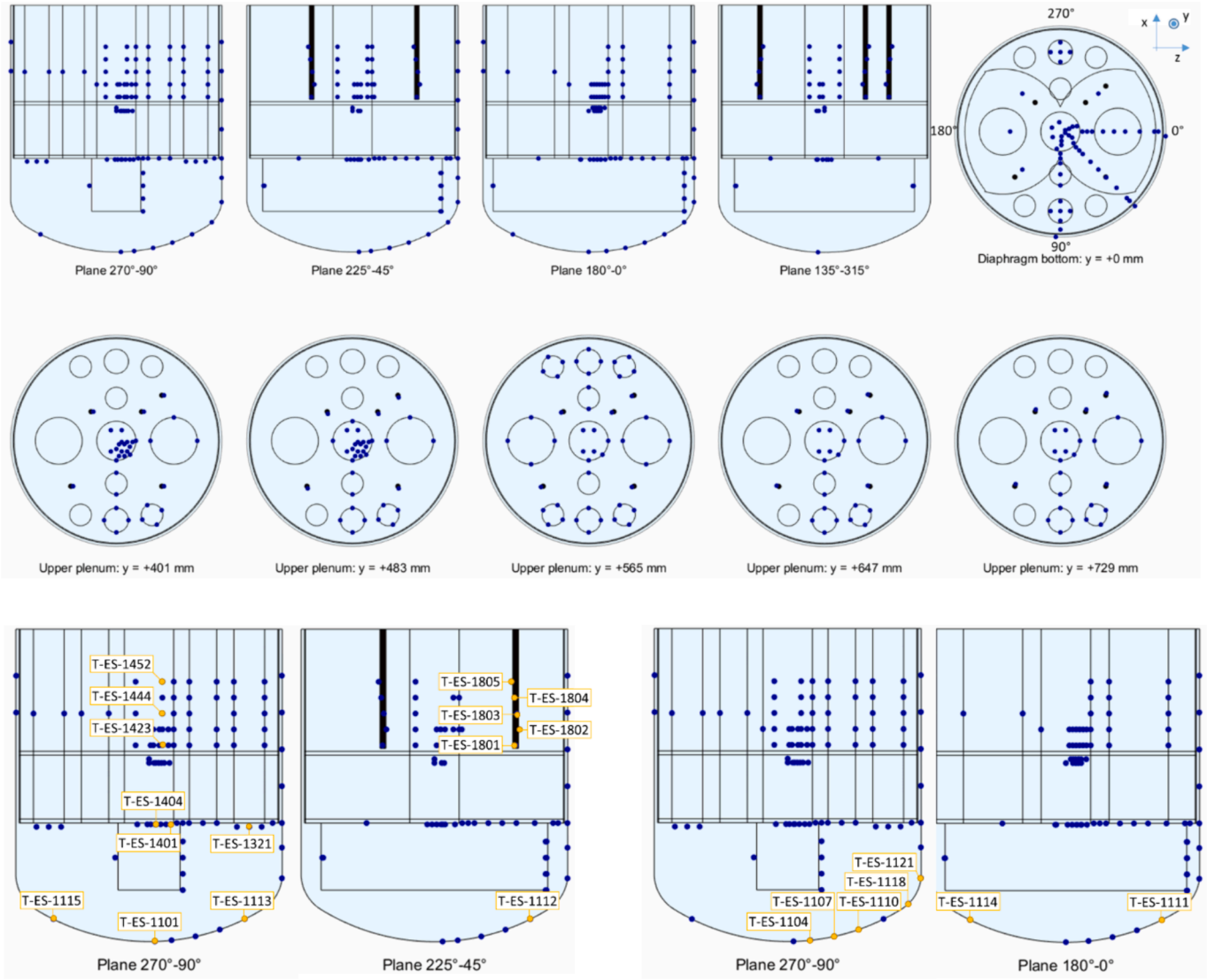

Fig. 4. Main vessel thermocouple positions including labels for selected thermocouples.

$$\Delta p_{core+ACS} = \rho_{LBE}.g.(l_{LP} - l_{UP}) \quad (44)$$

The LBE levels in the upper and lower plena (L-ES-1101/1701) are measured using two Rosemount 5300 Level Transmitters – Guided Wave Radar (standard accuracy ± 3.0 mm, relative accuracy after in-situ calibration < 0.3 mm).

A total of 320 thermocouples (TCs, type K with a stainless steel jacket, ∅ 1 mm, standard accuracy ± 1.5 K, relative accuracy after in-situ calibration < 0.7 K) are used to establish an LBE temperature map in the main vessel (see Fig. 4). The quarter section between 0° and 90° connected to circuit A hosts the most TCs in order to characterize in detail the motion of the hot plug. Asymmetry of the temperature map can be determined by TCs at specific elevations and in corresponding positions in each quadrant. TCs along vertical measurement rods A to E in the upper plenum indicate possible thermal stratification (see Fig. 3).

An additional 17 TCs (T-ES-2xx) are positioned in thermowells in the two external LBE circuits (type K, ∅ 1.5 mm, standard accuracy ± 1.5 K, relative accuracy after in-situ calibration < 0.7 K). The time response of the TCs in the thermowells is different from the TCs in the main vessel that are in direct contact with the LBE. The response of the bare TCs can be considered instantaneous, whereas the response of the TCs in the thermowell is delayed with a 1st order time constant τ_{well} of 6 s as measured by a dip test in LBE. All LBE TCs are calibrated in-situ with respect to reference thermocouple T-ES-208 in circuit A positioned before the entrance of the main vessel. Eight thermocouples (T-ES-3xx) in thermowells measure the temperature in the oil circuit (type K, ∅ 1.5 mm, standard accuracy ± 1.5 K).

The smallest time interval between two measurement data recordings is 300 ms. Process control parameters are recorded with a time interval of 60 s. In steady-state cases, all measurements are sampled over a sufficiently large period of time after steady flow conditions have been established (typically 20 min), to ensure that a sufficient amount of data is collected to perform statistical analysis. In addition to the statistical deviation σ_{stat}, the accuracy of the instrumentation σ_{inst} and the uncertainty due to analogue-to-digital conversion σ_{ADC} are taken into consideration. Results are presented here with their total uncertainty of $1 \times \sigma_{tot}$. For secondary variables, the uncertainty is propagated following the approach of Moffat (Moffat, 1988), assuming all contributions are independent from each other. Thermophysical properties of LBE and associated uncertainties are taken from (NEA, 2015).

The coordinate system used in this work is indicated in Fig. 3. Its origin in (x,z)-direction is at the center of the core simulator. In the vertical y-direction, the zero position is at the bottom of the lower diaphragm plate.

4. Test matrix

The test matrix for E-SCAPE includes the following six types of experiments:

1. *calibration cases* to calibrate the thermocouples and other instruments and to estimate the heat losses from the system;
2. *isothermal cases* mainly aimed at establishing the system hydraulic parameters such as pressure losses and free surface levels;
3. *hot-plug experiments*, using temperature as a tracer for flow, from which information can be obtained on residence times and flow mixing in the reactor plena;
4. *forced circulation cases* to study the thermal hydraulic behavior of the system for different combinations of power and flow rate;
5. *natural circulation cases* at different power levels, starting conditions and circuit pressure losses;
6. *transient cases*, including (partial) loss-of-flow, partial loss-of-heat-sink, etc.

In §5 of this paper, the results of selected isothermal and hot-plug experiments are presented. The other results will be discussed in forthcoming papers.

5. Experimental results

5.1. Isothermal operation

In the isothermal test cases, flow rates in the LBE loops are set at a prescribed value and controlled by the variable speed drive of the LBE pumps based on values measured with the Coriolis flow meters. The throttle valves in the forced circulation (FC) circuits are fully open. The LBE system is preheated to 180.0 °C using tape heaters on the vessel and circuits.

In isothermal operation, the focus is on the characterization of the pressure losses across the vessel components. Fig. 5 shows the pressure difference between a point in the lower plenum and a point in the upper plenum at the same axial level $\Delta p_{core+ACS}$ (PD-ES-1003) as function of the total flow rate. As expressed in Eq. (44), it should also be equal to the static head resulting from the level difference between the plena, named PD-DL. One can see that the correspondence is very good. Also shown in Fig. 5 are the pressure differences between the inlet and outlet of the main vessel, measured in the two circuits A and B (PD-ES-202 and PD-ES-252 respectively). As those latter include additional pressure losses from the HX inlet windows, pump outlets and pump and HX tubes, they are higher than PD-ES-1003. The values for both circuits are very close to each other as should be expected.

Extrapolating the pressure difference in the vessel to the total nominal flow rate of 116.58 kg/s leads to values of 217 and 227 mbar. These values are below the estimated values from the scaling study of $\Delta p_{vessel} =$ 432mbar (see Table 1). An in-depth investigation, combined with CFD analysis (Lopes et al., 2021), has clarified the discrepancy: an error was made in the arrangement of holes during the manufacturing of the lower core grid plate and this was not noticed during assembly. As it was impossible to replace the core grid plate, it was decided to compensate the lower losses in the core by increasing the pressure losses in the circuits and in this way maintaining Eu_L. One has to keep this in mind when upscaling the level difference measured in E-SCAPE: the result will be smaller than the expected level difference in MYRRHA. This has however only a very little effect on the velocity and temperature profiles.

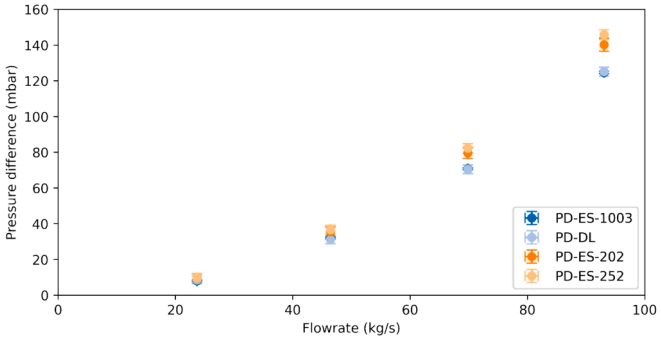

Fig. 5. Measured (PD-ES-1003) and calculated (PD-DL) pressure difference across the core and ACS, and pressure difference between vessel inlet and outlet for the circuit A (PD-ES-202) and circuit B (PD-ES-252) in forced circulation as function of the flow rate.

The LBE levels in the upper plenum and lower plenum are shown in Fig. 6. One can see that with increasing flow rate, the level in the upper plenum decreases while the one in the lower plenum increases. This is due to the increase of pressure loss in the core and ACS.

In the external circuits, one can use the isothermal tests to verify the hydraulic characteristics of different components. One of the important lessons learned from these tests is that the measured flow coefficient C_v of the throttle valves downstream the heat exchangers in circuit A are a factor 2 lower than the coefficients specified by the manufacturer. The resulting high pressure losses lead to audible cavitation in the valves at flow rates above 80 % of the nominal flow. Therefore, flow rates were limited to 80 % of the target design value in forced circulation in all experiments.

From the measured rotational speeds and the performance curves of the LBE pumps, the total pressure losses $\Delta p_{tot} = \Delta p_{vessel} + \Delta p_{pumpsandHXloops}$ in the system at the different flow rates can be estimated. Extrapolating these to 100 % of nominal flow, one obtains for loop A a value of 4604 mbar and for loop B 2339 mbar. Comparing these to the estimated forced-circulation value of 5002 mbar (see Table 1) shows that the throttle valves in both loops and especially in loop B need to be closed partially to respect the scaling. This will be important in natural circulation where buoyancy head and pressure loss need to be balanced.

5.2. Hot-plug experiments

The use of optical techniques to characterize flow paths or velocities in an opaque liquid is impossible. Other techniques for local velocity measurements in LBE (such as ultrasonic Doppler velocimetry) are very challenging, whereas temperature measurements are rather straightforward. Using temperature as a tracer, one can obtain information on flow paths and velocities from temperature measurements. In forced circulation, a 20 l hot plug can be inserted in circuit A upstream the inlet of the main vessel of E-SCAPE. Monitoring the response of thermocouples, information can be obtained on the possible presence of stagnant fluid regions (e.g. in the bottom or annular regions of the lower plenum), on the direction of the flow (e.g. upwards or radially in the upper plenum) and flow cycle times. From a code validation point of view, HP simulations allow to focus on the prediction of the momentum field independent of the effect of core heating.

Before the HP insertion, uniform temperature conditions at 180.0 °C are established in the primary system. In the HP section, the LBE temperature is raised to a value close to the target value of 250.0 °C. The speed of both LBE pumps is fixed, setting equal flow rates in both circuits and the total flow rate to 80 % or 20 % of the nominal flow. When the signal to actuate the three-way valve is given, the valve changes position in 5 s, inserting hot LBE in circuit A directly upstream the main vessel. Due to a very small change in pressure losses in circuit A when changing the valve position, there is a small change of flow rate in this circuit. The change remains below 4.0 % and 2.5 % of the desired flow rate for 80 % (Fig. 7 top) and 20 % of the nominal flow, respectively. The flow rate in circuit B remains unchanged.

5.2.1. HP insertion at high LBE flow rate

Thermocouples in the vessel and circuits are used to follow the HP motion. Fig. 7 shows the evolution of flow rates per circuit, the

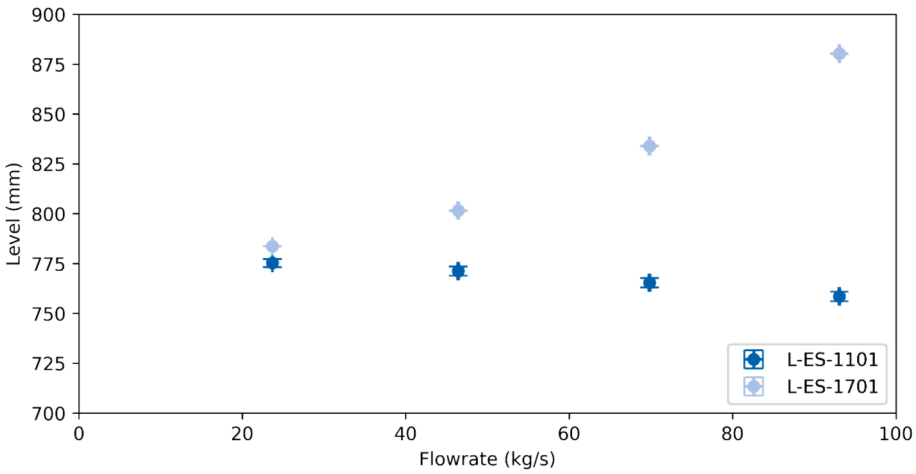

Fig. 6. LBE levels in the upper plenum (L-ES-1101) and the lower plenum (L-ES-1701) (bottom) in forced circulation as function of the flow rate.

LBE flow rates in circuit A (F-ES-201) and B (F-ES-251) and the hot plug (T-ES-207) and vessel inlet temperatures in circuit A (T-ES-208) and B (T-ES-257)	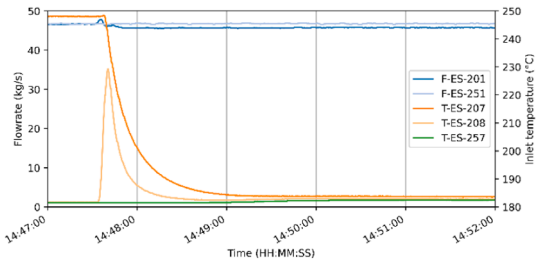
Temperatures along the anticipated flow path in the vessel	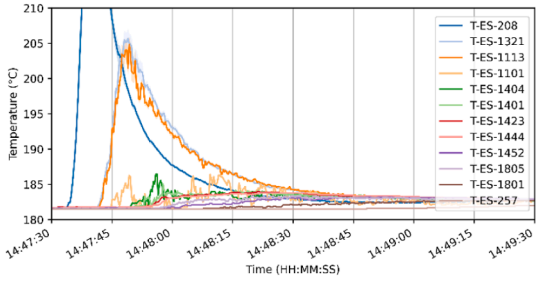
Vessel temperatures in a vertical plane cutting through the pumps	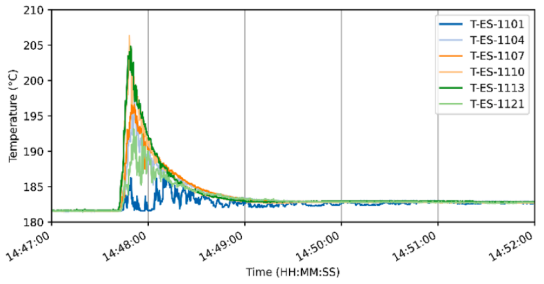
Temperatures in a horizontal plane cutting through T-ES-1113	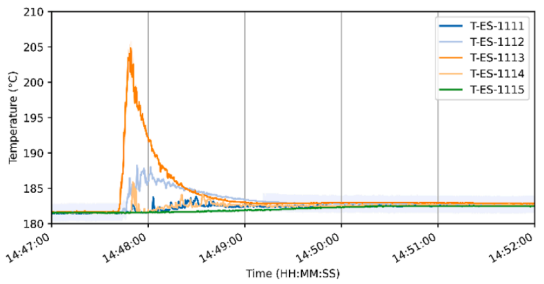

Fig. 7. Time evolution of LBE flow rates and temperatures for selected thermocouples during the hot plug transient at 80% flow rate.

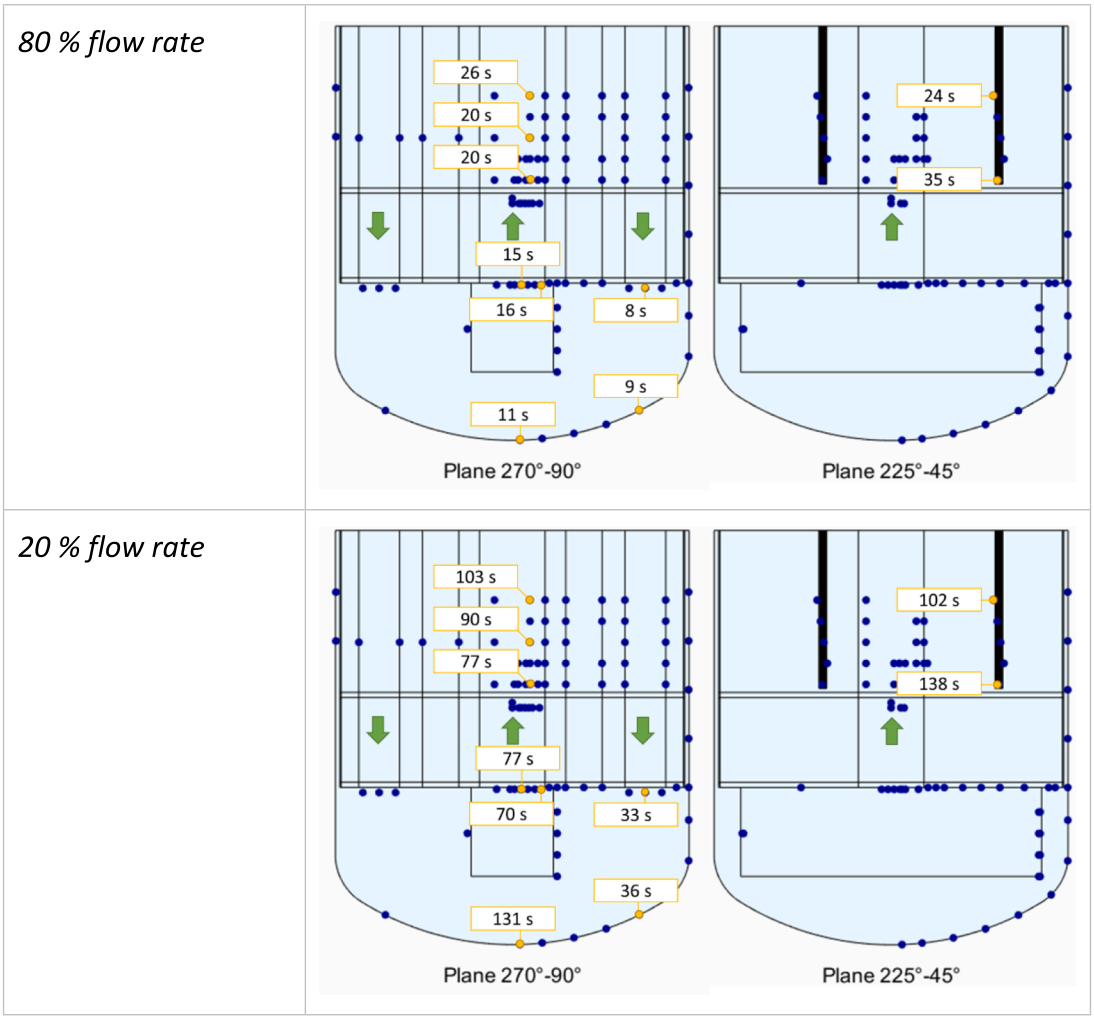

Fig. 8. Arrival time of the hot plug after the actuation of the three-way valve for a selected number of thermocouples during the hot plug transients at 80% and 20% flow rate.

temperatures in the HP section, the vessel inlet temperatures in circuit A and B and the temperatures in the vessel during the HP transient at 80 % flow rate. From the evolution of these quantities one can derive information on the flow cycle time through the system. T-ES-208 starts increasing 1 s after the three-way valve is actuated (marked by the change in flow rate in circuit A); T-ES-257 in circuit B starts increasing 75 s after the actuation. Hence, it takes about 74 s to complete the LBE flow cycle at 80 % flow rate.

The approximate arrival time of the hot plug Δt_{HP} after the actuation of the three-way valve can be registered at each individual thermocouple, as shown in Fig. 8 for a selected number of TCs. The TCs are chosen such that they represent the flow path through the primary vessel. Their position is indicated in Fig. 4.

- T-ES-1321 (located at the center of the pump channel right at the inlet of the lower plenum) is the first to see the hot plug arriving in the primary vessel, at $\Delta t_{HP} = 8$ s. It is located at a flow distance $\Delta s_{T-ES-208\rightarrow1321}$ of 4428 mm from T-ES-208. This leads to an approximate HP velocity in section between these TCs of 0.63 m/s.
- T-ES-1113 (at the vessel wall that is directly under T-ES-1321) sees the jet of the pump arriving at $\Delta t_{HP} = 9$ s. From the distance $\Delta s_{T-ES-1321\rightarrow1113}$, a jet velocity of 0.48 m/s can be derived.
- T-ES-1101 (at the bottom of the vessel in its center) is reached 2 s after the HP reaches T-ES-1113.
- T-ES-1404 and T-ES-1401 (respectively at the core inlet in the most central position and in the bypass region) are reached by the hot LBE reaches almost simultaneously at $\Delta t_{HP} = 15$ s and $\Delta t_{HP} = 16$ s.
- T-ES-1423 and T-ES-1444 (on one rod in the ACS at increasing elevations) are reached almost simultaneously, whereas it takes 6 s more to reach the highest T-ES-1452.
- T-ES-1805 (on measurement rod A at the same elevation as T-ES-1452) is reached 2 s before this TC at $\Delta t_{HP} = 24$ s.
- T-ES-1801 (mounted on measurement rod A at the same elevation as T-ES-1423) sees the hot LBE arriving quite a bit later than T-ES-1805 at $\Delta t_{HP} = 35$ s.

This evolution of temperature corresponds with the anticipated flow patterns in the lower and upper plena. From the time at which these TCs in the lower plena start increasing, one can derive that the pump jet hits the vessel after which the LBE flows along the vessel wall to the vertical center plane of the vessel cutting through the fuel handling machines (Plane 180° − 0°). Here the LBE turns upwards to the core. In the upper plenum one sees the LBE first going upwards through the ACS and spreading radially when it approaches the LBE free surface. From the free surface, it circulates downwards to the PHX inlets.

More lessons can be learned when looking in more detail to specific regions in the primary vessel. One can see how the pump jet first reaches the vessel right below the pump exit and then spreads radially. The third picture shows the evolution of temperatures in the symmetry plane

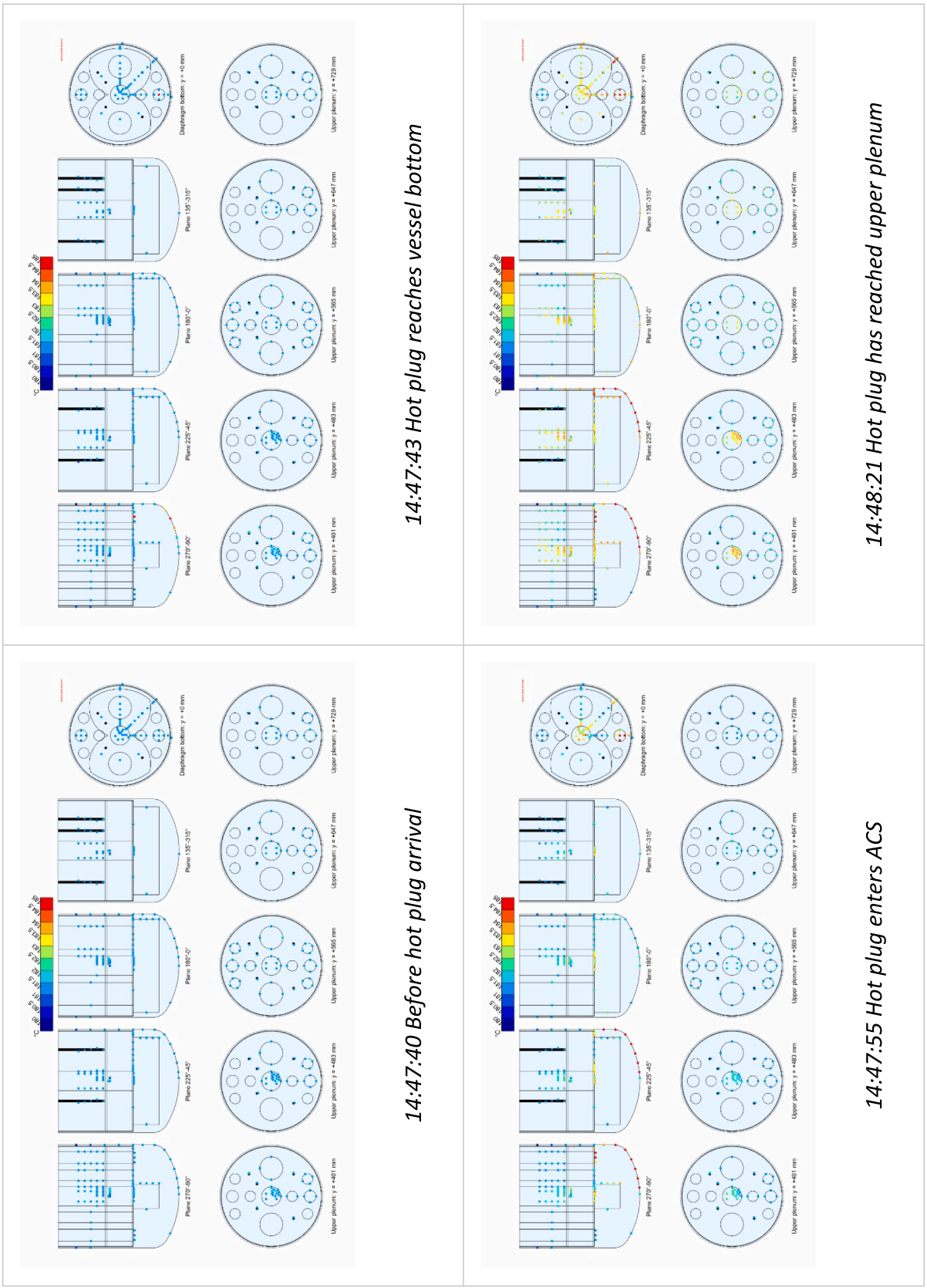

Fig. 9. Temperatures in the main vessel after hot plug insertion at 80% flow rate as function of time.

LBE flow rates in circuit A (F-ES-201) and B (F-ES-251) and the hot plug (T-ES-207) and vessel inlet temperatures in circuit A (T-ES-208) and B (T-ES-257)

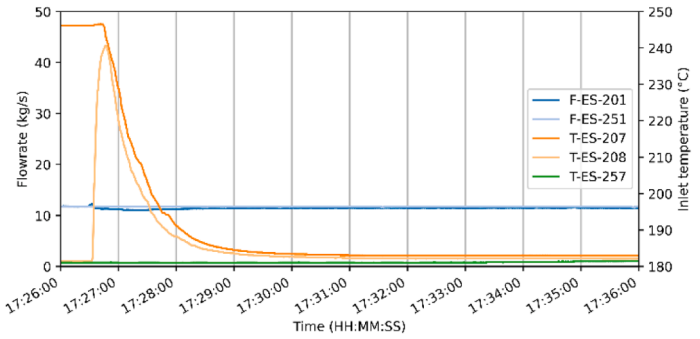

Temperatures along the anticipated flow path in the vessel

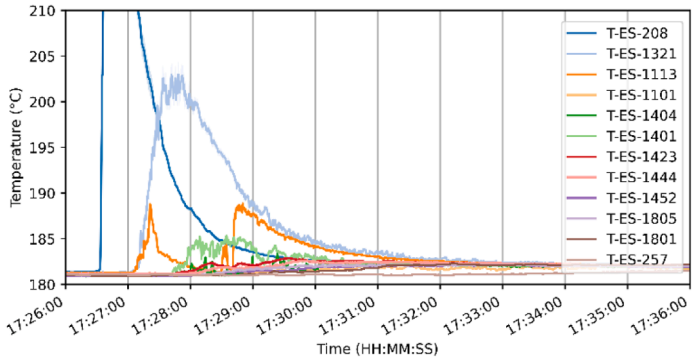

Vessel temperatures in a vertical plane cutting through the pumps

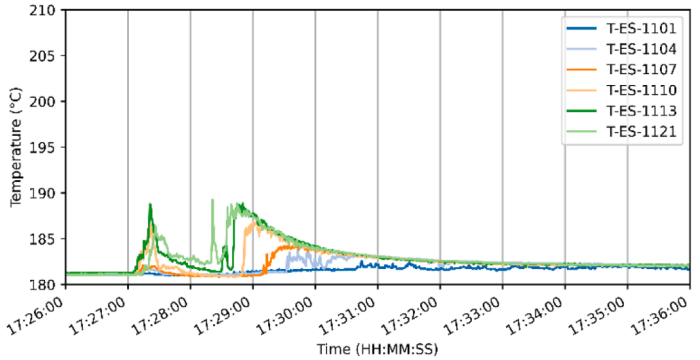

Temperatures in a horizontal plane cutting through T-ES-1113

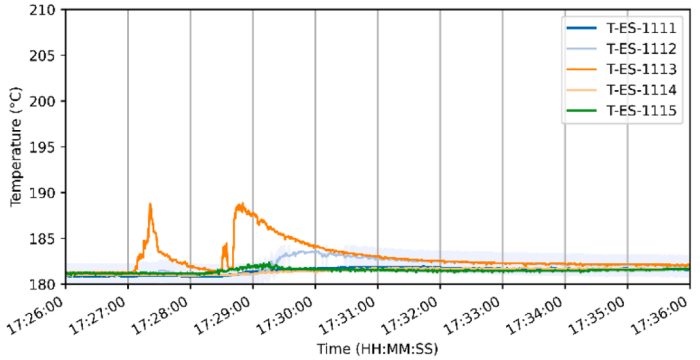

Fig. 10. Time evolution of the LBE flow rates and temperatures for selected thermocouples during the hot plug transient at 20% flow rate.

cutting through the pumps (Plane 270°–90°). The hot LBE moves towards the vessel bottom (T-ES-1113 → T-ES-1110 → T-ES-1107 → T-ES-1104 → T-ES-1101) on one side and curls upwards along the vessel wall (T-ES-1113 → T-ES-1121) on the opposite side. From the bottom picture showing the evolution of temperatures along the vessel wall in a horizontal plane on which T-ES-1113 is located, one can observe the jet spreading azimuthally as well (T-ES-1113 → T-ES-1112 → T-ES-1111/1114). The hot volume does not cross the 180°–0° symmetry plane to reach T-ES-1115.

Fig. 9 shows a series of temperature plots at moments in time from

which these flow patterns can be observed as well.

5.2.2. HP insertion at low LBE flow rate

Fig. 10 shows the evolution of the flow rates in both circuits combined with temperatures during the HP transient at 20 % flow rate. The change of flow rate in circuit A at the moment of the actuation of the three-way valve is now very limited. T-ES-208 starts increasing 3 s after the three-way valve is actuated; T-ES-257 starts increasing at about 292 s after the actuation. Hence, it takes about 289 s for the LBE to complete the flow cycle. This is a factor of 3.89 slower than at a flow rate of 80 % and approaches the factor of 4 in flow rate.

If one now tracks the same TCs as for the 80 % flow rate case (see Fig. 8), the following observations can be made:

- T-ES-1321 sees the hot plug arriving in the primary vessel first at 33 s after the actuation. This leads to a hot plug velocity in the pump tube between T-ES-208 and T-ES-1321 of 0.15 m/s, a factor of 4.29 lower than in the 80 % flow rate case.
- T-ES-1113 sees a first increase in temperature at $\Delta t_{HP} = 36$ s. From this, a jet velocity of 0.16 m/s can be calculated, which is close to the hot plug velocity in the pump tube. One can also notice that after this first jump in temperature, T-ES-1113 experiences a second increase in temperature about 90 s later, pointing towards recirculation of LBE in the lower plenum.
- In contrast to the 80 % flow rate case, it takes a long time before the temperature at the bottom of the vessel T-ES-1101 starts rising ($\Delta t_{HP} = 131$ s). The TC does not seem to be reached directly by the pump jet.
- T-ES-1401 and T-ES-1404 indicate rising temperatures 61 s before T-ES-1101 and about 37 s after the hot plug enters the lower plenum. T-ES-1401 responds 7 s before T-ES-1404.
- On the same rod in the ACS, it now takes much longer for the LBE to reach the higher TCs: T-ES-1423 ($\Delta t_{HP} = 77$ s), T-ES-1444 ($\Delta t_{HP} = 90$ s) and T-ES-1452 ($\Delta t_{HP} = 103$ s).
- T-ES-1805 is reached 1 s before T-ES-1452. T-ES-1801 sees the hot LBE arriving 36 s later than T-ES-1805.

The ratio of Δt_{HP} between the 80 % and 20 % flow rate cases is close to the expected value of 4 for all TCs except for T-ES-1101. From these observations, one can conclude that the flow pattern in the lower plenum is different for the 20 % flow rate case. The jet entering the lower plenum has less inertia and spreads radially much faster. It does not seem to penetrate as fast to the bottom of the vessel but turns towards the core at a much earlier stage. Here it reaches the bypass region before it reaches the center of the core. Also, there appears to be a recirculation in the lower plenum which re-entrains hot LBE into the pump jet, about 90 s after the first temperature peak is registered by T-ES-1113.

One can see how the pump jet reaches the vessel right below the pump exit and then spreads radially but with a large time delay and at much lower temperature levels than for 80 % flow rate. The hot LBE moves towards the vessel bottom and reaches T-ES-1113 and T-ES-1110 almost simultaneously. It spreads radially towards the center (T-ES-1113/1110 → T-ES-1107 → T-ES-1104), however without really reaching the central T-ES-1101. It curls upwards along the vessel wall (T-ES-1113 → T-ES-1121). All TCs experience a second jump in temperature. This could point towards flow recirculation in the lower plenum, possibly enhanced by buoyancy effects in the hot plug. From the bottom picture, one cannot observe azimuthal spreading in this case.

6. Conclusions

In this paper, the scaling approach for the E-SCAPE facility at SCK CEN is reported, together with the experimental results from its isothermal operation. E-SCAPE is a thermal hydraulic 1/6-scale model of the primary system of the MYRRHA reactor, with an electrical core simulator, cooled by LBE.

The scaling approach for E-SCAPE is based on the preservation of the overall system behavior and the reproduction of the major thermal hydraulic phenomena under decay heat removal conditions. In natural circulation, the similarity of the steady-state integral system behavior is realized by respecting Richardson, Euler and Heat Source number similarity. In forced circulation, Richardson similarity is no longer required. Specific attention in the scaling approach is given to stratification phenomena in the upper plenum and the mixing effect associated with jets entering the plena.

Important to note is that in E-SCAPE, in contrast to MYRRHA, pumps and heat exchangers are in external circuits connected to the primary vessel. These external circuits have been designed, however, to provide the correct boundary conditions to the primary vessel, both in forced and natural circulation steady-state conditions. In transient conditions, one has to take into account the additional (thermal) inertia of the LBE-filled circuits and the time it takes for the coolant to pass through these circuits when assessing the evolution of the system in time.

From steady-state isothermal operation, experimental information is given on the pressure losses in the main vessel and the external circuits. The relation between the pressure loss in the core and ACS, and the level difference between the lower and upper plenum is confirmed.

Discrepancies between the measured pressure losses and the targeted scaled values in the main vessel and the circuits can be attributed to manufacturing issues. Larger pressure losses in the circuits limit the experimental flow rates to 80 % of the nominal value in forced circulation. Smaller pressure losses over the core result in a smaller level difference between the upper and lower plena. Their effect on the velocity and temperature profiles is very small. The total system pressure loss, important in natural circulation, can be set to the desired value using throttle valves.

From the hot plug experiments, using temperature as a flow tracer, one can obtain a substantial amount of information on the flow patterns in forced circulation mode without actually measuring velocities. One can observe the pump jets entering in the lower plenum and see a clear difference in their behavior between the high and low flow rate cases with respect to their penetration and radial distribution. Moreover, it is observed that the LBE does not cross the vertical symmetry plane cutting through the fuel handling machines in the lower plenum and that it does go upwards along the vessel walls into the gap between the diaphragm and the vessel. In the low flow rate case, recirculation is observed in the lower plenum. One can also see that the LBE that exits the core, is going upwards through the ACS before distributing radially in the uppermost fluid layers. From these layers, the fluid goes downward in the upper plenum towards the HX inlet windows.

In order to fully understand the flow patterns and explain the temperature evolution in certain positions, CFD simulations of the hot plug cases are very valuable. Vice versa, the hot plug experiments provide a wealth of data for code validation. Pre-test simulations of the hot plug experiments have been performed to support the design of the facility (Van Tichelen et al., 2015). Post-test simulations are the topic of ongoing activities. The combined experimental and numerical efforts will provide information on the flow mixing that can be directly extrapolated to MYRRHA.

CRediT authorship contribution statement

Katrien Van Tichelen: Writing – original draft, Methodology, Investigation, Formal analysis, Conceptualization. **Fabio Mirelli:** Writing – review & editing, Software, Methodology, Investigation. **Matteo Greco:** Writing – review & editing, Methodology. **Yann Bartosiewicz:** Writing – review & editing, Supervision. **William D'haeseleer:** Writing – review & editing, Supervision.

Declaration of competing interest

The authors declare that they have no known competing financial

interests or personal relationships that could have appeared to influence the work reported in this paper.

Data availability

The authors do not have permission to share data.

Acknowledgements

We wish to express our great appreciation for and acknowledge the craftsmanship of the LBE-CE, DEO, HWP and NEO teams at SCK CEN in the design, construction and commissioning of E-SCAPE. We would also like to thank our colleagues from the von Karman Institute for Fluid Dynamics for their excellent work on MYRRHABELLE.

This work was partially supported by the Research and Innovation Action MYRTE – MYRRHA Research and Transmutation Endeavour, co-funded by the European Union H2020 program under grant agreement n°662186.

Appendix A. Supplementary data

Supplementary data to this article can be found online at https://doi.org/10.1016/j.nucengdes.2024.113361.

References

Aït Abderrahim, H., 2011. MYRRHA Technical Description. SCK CEN, Mol.

Aït Abderrahim, H., De Bruyn, D., Van den Eynde, G., Fernandez, R., 2021. Accelerator driven subcritical systems. In: Encyclopedia of Nuclear Energy. Elsevier, pp. 191–202. https://doi.org/10.1016/b978-0-12-819725-7.00093-3.

De Bruyn, D. (2021, 2). Development of advanced reactor systems: the MYRRHA project. *SNETP Forum 2021.* SNETP.

Duratherm. (2023). *Duratherm Heat Transfer Fluids.* Retrieved 3 21, 2023, from https://durathermfluids.com/products/duratherm-hf/?/heat-transfer-fluid/duratherm-hf/.

Eguchi, Y., Takeda, H., Koga, T., Tanaka, N., Yamamoto, K., 1997. Quantitative prediction of natural circulation in an LMFR with a similarity law and a water test. Nucl. Eng. Des. 178, 295–307. https://doi.org/10.1016/S0029-5493(97)00234-3.

European Commission. (2015). *MYRTE, Euratom H2020.* Retrieved 3 21, 2023, from https://cordis.europa.eu/project/id/662186.

Grewal, S., Gluekler, E., 1982. Water simulation of sodium reactors. Chem. Eng. Commun. 17, 343–360. https://doi.org/10.1080/00986448208911637.

Guenadou, D., Aubert, P., Descamps, J.-P. 2021. Gas entrainment in the mock-up of the upper plenum of a sodium cooled reactor. Nucl. Eng. Des., *383*, 111448. doi:10.1016/j.nucengdes.2021.111448.

Guenadou, D., Tkatschenko, I., Aubert, P., 2015. Plateau facility in support to ASTRID and the sfr program: an overview of the first mock-up of the ASTRID upper plenum, MICAS. *NURETH16 - 16th International Topical Meeting on Nuclear Reactor Thermal Hydraulics*.

IAEA. 2013. *Benchmark Analyses on the Natural Circulation Test Performed During the Phenix End-Of-Life Experiments: IAEA Tecdoc Series No. 1703.* IAEA.

IAEA. 2017. *Benchmark analysis of EBR-II shutdown heat removal tests: IAEA Tecdoc Series No. 1819.* IAEA.

Ieda, Y., Kamide, H., Ohshima, H., Sugawara, S., Ninokata, H. 1993. Strategy of experimental studies in PNC on natural convection decay heat removal. *IAEA-IWGFR Specialists' Meeting on Evaluation of Decay Heat Removal by Natural Convection.* IAEA.

Ieda, Y., Maekawa, I., Muramatsu, T., Nakanishi, S., 1990. 6). Experimental and analytical studies of the thermal stratification phenomenon in the outlet plenum of fast breeder reactors. Nucl. Eng. Des. 120, 403–414. https://doi.org/10.1016/0029-5493(90)90390-j.

Ishii, M., Kataoka, I., 1984. Scaling laws for thermal-hydraulic system under single phase and two-phase natural circulation. Nucl. Eng. Des. 81, 411–425. https://doi.org/10.1016/0029-5493(84)90287-5.

Ishii, M., Revankar, S.T., Leonardi, T., Dowlati, R., Bertodano, M.L., Babelli, I., Han, J.T., 1998. The three-level scaling approach with application to the Purdue University Multi-Dimensional Integral Test Assembly (PUMA). Nucl. Eng. Des. 186, 177–211. https://doi.org/10.1016/S0029-5493(98)00222-2.

Lopes, S., Koloszar, L., Planquart, P., Visser, D. C., Van Tichelen, K. 2021. Hunting for the correct pressure drop in a scaled reactor pool: Effect of geometry, mesh resolution, turbulence model and mass flow. Nucl. Eng. Des., *384*, 111452. doi:10.1016/j.nucengdes.2021.111452.

Lorenz, J. J., Howard, P. A. 1977. Study of the density interface in a stratified LMFBR outlet plenum. In: *AIChE/ASME Heat transfer Conference.* ASME.

Lorusso, P., Del Nevo, A., Narcisi, V., Giannetti, F., Caruso, G., Zwijsen, K., Tarantino, M., 2021. Total loss of flow benchmark in CIRCE-HERO integral test facility. Nucl. Eng. Des. 376, 111086 https://doi.org/10.1016/j.nucengdes.2021.111086.

Mente, V.M., Pandey, G.K., Banerjee, I., Kumar, S.A., Padmakumar, G., Rajan, K.K., 2014. Experimental studies in water for safety grade decay heat removal of prototype fast breeder reactor. Ann. Nucl. Energy 65, 114–121. https://doi.org/10.1016/j.anucene.2013.10.017.

Moffat, R.J., 1988. Describing the uncertainties in experimental results. Exp. Therm Fluid Sci. 1, 3–17. https://doi.org/10.1016/0894-1777(88)90043-X.

Murakami, T., Eguchi, Y., Oyama, K., Watanabe, O., 2015. Reduced-scale water test of natural circulation for decay heat removal in loop-type sodium-cooled fast reactor. Nucl. Eng. Des. 288, 220–231. https://doi.org/10.1016/j.nucengdes.2015.04.007.

NEA. (2015). *Handbook on Lead-Bismuth Eutectic Alloy and Lead Properties, Materials Compatibility, Thermal-Hydraulics and Technologies* (2 ed.). Nuclear Energy Agency. doi:10.1787/42dcd531-en.

Ono, A., Kurihara, A., Tanaka, M., Oshima, H., Kamide, H., Miyake, Y., Nakane, S., 2017. Study on reactor vessel coolability of sodium-cooled fast reactor under severe accident condition. Water experiments using a scale model. Proceedings of 2017 International Congress on Advances in Nuclear Power Plants (ICAPP2017).

Peterson, P.F., 1994. Scaling and analysis of mixing in large stratified volumes. Int. J. Heat Mass Transf. 37, 97–106. https://doi.org/10.1016/0017-9310(94)90013-2.

Peterson, P.F., Schrock, V.E., Greif, R., 1998. Scaling for integral simulation of mixing in large, stratified volumes. Nucl. Eng. Des. 186, 213–224. https://doi.org/10.1016/S0029-5493(98)00223-4.

Planquart, P., Van Tichelen, K., 2019. Experimental investigation of accidental scenarios using a scale water model of a HLM reactor. Nucl. Eng. Des. 346, 10–16. https://doi.org/10.1016/j.nucengdes.2019.02.016.

Takeda, H., Koga, R., Watanabe, O., 1993. Experimental and computational simulation for natural circulation in an LMFBR. Nucl. Eng. Des. 140, 331–340. https://doi.org/10.1016/0029-5493(93)90116-q.

Tanaka, N., Moriya, S., Ushijima, S., Koga, T., Eguchi, Y., 1990. Prediction method for thermal stratification in a reactor vessel. Nucl. Eng. Des. 120, 395–402. https://doi.org/10.1016/0029-5493(90)90389-F.

Tenchine, D., 2010. Some thermal hydraulic challenges in sodium cooled fast reactors. Nucl. Eng. Des. 240, 1195–1217. https://doi.org/10.1016/j.nucengdes.2010.01.006.

Van Tichelen, K., Mirelli, F., Greco, M., Viviani, G., 2015. E-SCAPE: A scale facility for liquid-metal, pool-type reactor thermal hydraulic investigations. Nucl. Eng. Des. 290, 65–77. https://doi.org/10.1016/j.nucengdes.2014.11.011.

Vidil, R., Grand, D., Leroux, F., 1988. Interaction of recirculation and stable stratification in a rectangular cavity filled with sodium. Nucl. Eng. Des. 105, 321–332. https://doi.org/10.1016/0029-5493(88)90253-1.

Weinberg, D., Rust, K., Hoffmann, H., 1996. Overview Report of RAMONA-NEPTUN Program on Passive Decay Heat Removal. Tech. rep. Forschungszentrum Karlsruhe.